Single-channel analysis of the anion channel-forming protein from the plant pathogenic bacterium *Clavibacter michiganense ssp. nebraskense*

Theo Schürholz, Larissa Dloczik, and Eberhard Neumann
Faculty of Chemistry, Bielefeld University, D-4800 Bielefeld 1, Germany

ABSTRACT The anion channel protein from *Clavibacter michiganense ssp. nebraskense* (Schürholz, Th. et al. 1991, *J. Membrane Biol.* 123: 1–8) was analyzed at different concentrations of KCl and KF. At 0.8 M KCl the conductance $G(V_m)$ increases exponentially from 21 pS at 50 mV up to 53 pS at V_m = 200 mV, 20°C. The concentration dependence of $G(V_m)$ corresponds to a Michaelis–Menten type saturation function at all membrane voltage values applied (0–200 mV). The anion concentration $K_{0.5}$, where $G(V_m)$ has its half-maximum value, increases from 0.12 M at 50 mV to 0.24 M at 175 mV for channels in a soybean phospholipid bilayer. The voltage dependence of the single channel conductance, which is different for charged and neutral lipid bilayers, can be described either by a two-state flicker (2SF) model and the Nernst–Planck continuum theory, or by a two barrier, one-site (2B1S) model with asymmetric barriers. The increase in the number of open channels after a voltage jump from 50 mV to 150 mV has a time constant of 0.8 s. The changes of the single-channel conductance are much faster (<1 ms). The electric part of the gating process is characterized by the (reversible) molar electrical work $\Delta G^{\ominus}_{el} = \rho z_g F V_m \approx -1.3$ RT, which corresponds to the movement of one charge of the gating charge number $|z_g| = 1$ across the fraction $\rho = \Delta V_m / V_m = 0.15$ of the membrane voltage V_m = 200 mV. Unlike with chloride, the single channel conductance of fluoride has a maximum at about 150 mV in the presence of the buffer PIPES (≥5 mM, pH 6.8) with $K_{0.5} \approx 1$ M. It is shown that the decrease in conductance is due to a blocking of the channel by the PIPES anion. In summary, the results indicate that the anion transport by the *Clavibacter* anion channel (CAC) does not require a voltage dependent conformation change of the CAC.

INTRODUCTION

The *Corynebacterium Clavibacter michiganense ssp. nebraskense* causes Goss's wilt and blight in *Zea mais* (1). Members of the genus *Clavibacter* have been described to produce phytotoxins which were classified as high molecular mass polysaccharides (*C. m. ssp. michiganense;* (2)) or glycolipids (*C. rathayi;* (3)). The isolated polysaccharides cause wilting in plant assays (4) and a degeneration of chloroplasts (5). However, such an effect can be attributed to water stress rather than to a discrete action of the polysaccharide on the chloroplasts and its membrane. During a systematic search for toxic activities excreted into the culture medium by *C. m. ssp. nebraskense* we have identified a membrane-active component which forms anion channels in planar lipid bilayers (6) and is therefore called the *Clavibacter* anion channel (CAC).

The CAC inserts spontaneously into planar lipid membranes when culture fluid of this species is added to the aqueous phase of the bilayer chamber. Channel activity can be abolished by protease treatment of the planar bilayer (6). The relative molecular mass of the CAC is $M_r \sim 25{,}000$ as determined by functional reconstitution of the channel protein from SDS gels (data will be published in a separate paper). The channels can be blocked by indanyloxyacetic acid (IAA-94) and by OH^--ions (pH > 10) (6). The channels formed are highly anion-selective. The conductance decreases with increasing crystal radius of the halides, which are larger than Cl^-. The CAC is also permeable for small inorganic and organic anions, which do not contain methyl groups, and is impermeable for gluconate. The channels show a unique voltage dependence: (*a*) The single channel conductance increases linearly with voltage up to 200 mV, saturating at 250 mV with 25–30 pS (300 mM KCl). The channel is closed at negative voltage relative to the side of CAC insertion (diode type *I–V*-curve). (*b*) The average number of open channels also increases with voltage (6). The voltage dependent conductance of the channel, at different anion concentrations and in the presence of ion gradients, is analyzed in terms of the Nernst–Planck continuum theory and the reaction rate theory. The results indicate that the voltage dependent anion transport does not require a voltage dependent conformational change of the CAC.

MATERIALS AND METHODS

CAC preparation. The strain *Clavibacter michiganense ssp. nebraskense* (NCPPB 2581) was obtained from the National Collection of Plant Pathogenic Bacteria, Hatching Grenn Harpenden, England. Culture conditions and purification of the CAC were performed as described in (6).

Voltage clamp measurements. The chemicals used in the bilayer experiments were all of analytical grade. The planar lipid bilayer chambers contained 300 mM KCl and 5 mM PIPES (pH 6.8, 20°C) as a standard solution. Exchange of the aqueous solutions was performed by the aid of two syringes (5–10 chamber volumes) and under continuous stirring. Planar bilayers (diameter ~ 0.1 mm) were obtained by apposition of two vesicle derived monolayers (7). Vesicles were formed from total soybean phospholipids (20% lecithin; Avanti Polar Lipids Inc., Birmingham, AL) with 10% (wt) cholesterol (lipid C) or soybean lecithin (>95%) with 30% (wt) cholesterol (lipid N). The lipid was deposited as a thin film in a round bottom flask by chloroform evaporation (rotavap) and subsequently suspended in 80 mM HEPES

Address correspondence to Dr. Theo Schürholz, Fakultät für Chemie, Universität Bielefeld, Postfach 8640, D-4800 Bielefeld 1, Germany.

0006-3495/93/01/058/10 $2.00

(pH 7) to a final concentration of 30–50 mg/ml by shaking with small glass beads. The suspension was homogenized by 1-min sonication in a bath and additional 3–4 freeze-thaw steps. The vesicles were stored at −80°C and were diluted 10–20 times in the appropriate salt solution before addition to the bilayer chambers (~100 μl to each). For all current measurements, a current to voltage converter was used with an OPA-104CM amplifier (Burr & Brown Instrumentation, Inc., Tucson, AZ) and a 10^{10} Ω feedback resistor. The *trans* side of the bilayer chamber was connected to virtual ground (ϕ_{trans}). The voltage V_m is given by

$$V_m = \phi_{cis} - \phi_{trans} \quad (1)$$

and thus refers to the electric potential (ϕ_{cis}) on the *cis* side, where the CAC was added (For details of current direction, electrical potential difference ($\Delta\phi$), and voltage $V_m = -\Delta\phi$ see also Fig. 6). The current measurements were performed at 20°C. Data were stored on a videotape recorder and analyzed by the aid of a computer oscilloscope (Erhard Bablock, Augsburg, FRG) after filtering with a 4-pole Bessel filter at 100–1000 Hz. The current amplitude was determined from the digitized data (average of ten channels).

RESULTS

Voltage dependence of the single channel conductance. In Fig. 1 typical channel traces of the CAC are shown, which was incorporated into a planar bilayer. The solutions on the *trans*- and on the *cis*-side contained 1 M KCl (*A*) or 1 M KF (*B*), respectively. The open channel events were separated by closing gaps ranging from 100 ms to below 1 ms. The noise in the open state was large, compared to that of the closed state, indicating that the open channels fluctuated between conformational substates of different conductance. Even at 1 kHz, the maximal resolution of the amplifier, such substates could not be resolved. The average open and closed times of these fluctuations, therefore, should be correspondingly shorter. The channel noise increased with increasing membrane voltage and was especially large in the presence of F^- as the permeant ion.

The current (I) and the conductance (G) of the single channel event could be formally described by an exponential function of the membrane-voltage V_m:

$$I = V_m \cdot G(V_m, a) \quad \text{and} \quad (2)$$

$$G(V_m, a) = G_0(a) \cdot \exp(bV_m), \quad (3)$$

where $G_0(a)$ is the conductance at $V_m = 0$, a is the activity of the permeant anion, and b is a constant. In Fig. 2 it is seen that at the highest V_m-values applied, the measured current values were slightly lower than the value of the corresponding curve, which was fitted with Eqs. 2 and 3. Both, the intercept and the slope of the conductance curves $G(V_m)$ increased, when the Cl^--concentration was raised (Fig. 2 *B, D,* and Table 1). The conductance values of the anion channel were generally lower in the neutral lipid membrane (lipid N), containing 46 mol% cholesterol, than in the membranes with 30 mol% negatively charged lipids (lipid C). In contrast to all other anions, the F^--conductance at first increased up to 150 mV and then decreased with increasing voltage (Fig. 2 *F*). It was found that this effect depended on the concentration of the buffer (PIPES), which obviously acts as a (weak) channel blocker. The conductance value G_0 = 19 pS at 1 M KF was comparable to G_0 = 18 pS for KCl, as estimated from Fig. 2 *B*. The initial slope of the F^--conductance curves was independent of the KF concentration. The buffer reduced the chloride conductance only at high concentrations and had no measurable effect at ≤5 mM (Table 2).

Dependence of the conductance on the ion concentration. In Fig. 3 it is shown that the conductance increased as a function of the activity a(KCl). The measured G-values can be described by a saturation function of Michaelis–Menten type,

$$G(V_m, a) = G_{max}(V_m) \cdot \frac{a}{K_{0.5}(V_m) + a}, \quad (4)$$

where $G_{max}(V_m)$ is the maximum conductance at a given V_m-value and $K_{0.5}$ is the activity, at which the conductance reaches half the maximum value. The G_{max}-values, which were obtained for lipid C and lipid N, were only slightly different. Specifically, between 50 and 175 mV, $G_{max,C}$ ranged from 27–71 pS and $G_{max,N}$ from 30–73 pS. The corresponding $K_{0.5}$-values were between 0.12 and 0.24 M and between 0.25 and 0.33 M, respectively. The single values were summarized in Table 3.

Salt gradients. The current intensities of the Cl^--channels in the presence of salt gradients are shown in Fig. 4. At 100 mM KCl on the *cis*-side and 1 M KCl on the *trans*-side the gradient was called (+)gradient, because the resulting changes in current were positive; the reverse gradient was called (−)gradient. The current data could be adequately described by the Goldman–Hodgkin–Katz (GHK)-current equation (8), when the voltage dependence of the conductance was taken into account. The GHK-equation for the current $I = I_{Cl}$ with $z = z_{Cl} = -1$, is:

$$I = V_m \cdot P_{Cl} A \cdot uF \times \frac{a(Cl^-, cis) - a(Cl^-, trans) \cdot \exp(uV_m)}{1 - \exp(uV_m)}, \quad (5)$$

where P_{Cl} is the permeability coefficient of chloride, A is the apparent cross-section of the pore, F is the Faraday constant, R is the gas constant, T the Kelvin temperature, and $u = F/RT$. Since the permeability and the area of ionic channels can hardly be determined separately, we preferred to use the conductance instead. Comparing Eqs. 5 and 2, it can be seen that $G(V_m, a) = P_{Cl} A \cdot uF \cdot a(Cl^-)$ and Eq. 5 can be rewritten as

$$I = V_m \cdot \frac{G_0(a)}{a(Cl^-)} \cdot \exp(bV_m) \times \frac{a(Cl^-, cis) - a(Cl^-, trans) \cdot \exp(uV_m)}{1 - \exp(uV_m)}. \quad (6)$$

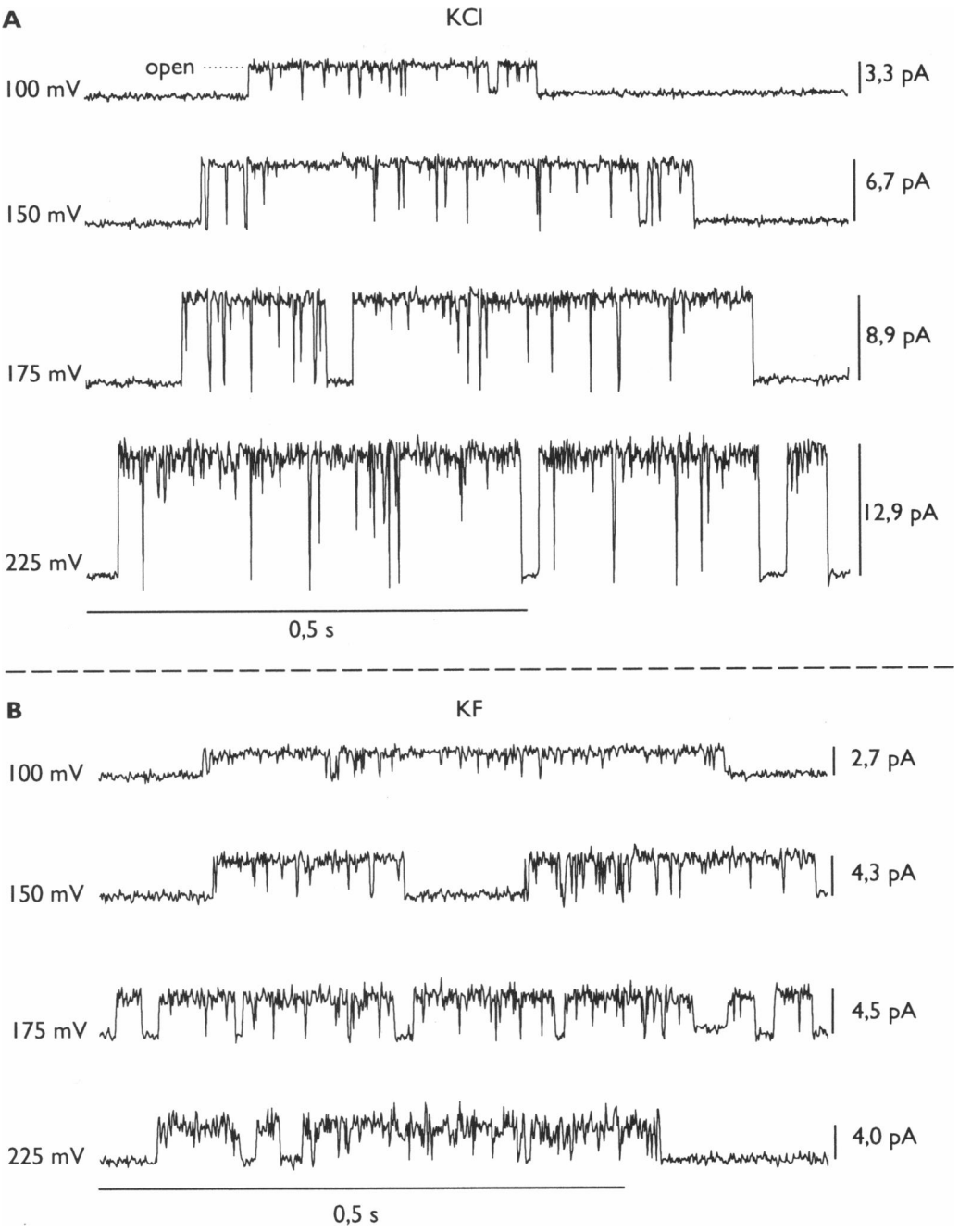

FIGURE 1 Channel traces $I(t)$, of the *Clavibacter* anion channel (CAC) in 1 M KCl and in 1M KF at four transmembrane voltages V_m. Standard buffer was 5 mM Pipes, pH 6.8, 20°C. The recordings were filtered with a 4-pole Bessel filter at 1 kHz. The CAC was added from the *cis*-side of the membrane. The membrane voltage is defined as $V_m = \phi_{cis} - \phi_{trans}$; channels open upward. See Eqs. 1 and 2 of the text.

Eq. 6 was used to describe the current data, which were measured in the presence of KCl-gradients. The continuous curves in Fig. 4 were calculated, taking the term $G_0(a)/a(Cl^-) = G_0(a)/a(Cl^-, trans)$ as constant. The value of this term was obtained from the corresponding measurements under symmetric ionic conditions $a(Cl^-, cis) = a(Cl^-, trans)$. Although finite current values were expected from theory, no single-channel events were detected at $V_m = 0$ with either of the gradients applied.

Voltage jump measurements. To analyze the kinetics of the voltage dependent changes of the chloride channel, voltage steps were applied from 50 to 150 mV and vice versa (Fig. 5). Two main relaxation phases could be distinguished. The rapid phase (I), which was hidden in the capacitive transient, could not be resolved on the time scale of 1 ms. As judged from voltage jump experiments with single channels (data not shown) phase (I) contained the increase of the single-channel conduc-

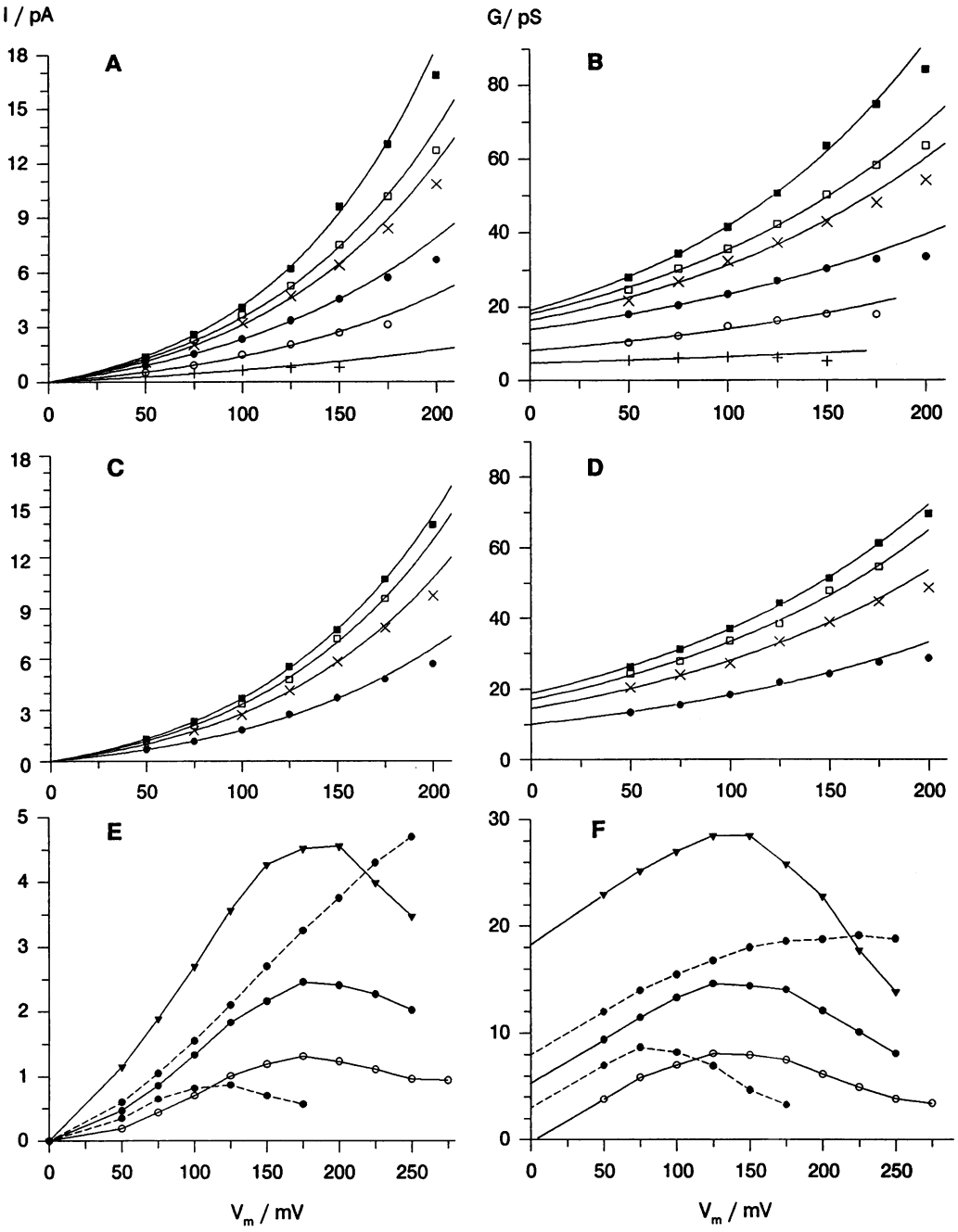

FIGURE 2 Current (I) and conductance (G) as a function of voltage (V_m) at various anion activities. The data were fitted according to Eqs. 2 and 3; see also Table 1. (A), (B), (C), (D) refer to KCl, (E), (F) to KF; anion concentrations: + 0.03 M; ○ 0.1 M; ● 0.3 M; × 0.8 M; ▼ 1 M; □ 1.8 M; ■ 3 M. The broken lines refer to 0.5 mM (upper) and 100 mM PIPES (lower), respectively. The planar membrane was made from charged lipids "C" (A), (B), (E), (F) and neutral lipids "N" (C), (D). See the legend to Fig. 1 and the text.

tance of already open channels (in addition to the ohmic part of the current increase). Hence, the slower phase (II) most likely represented an increase in the average number of open channels. Within the experimental error margin, the slow process could be fitted by one exponential with a time constant τ(II, 150 mV) = 0.8 s. The relaxation time for the decrease of current (phase II) was τ(II, 50 mV) = 0.3 s.

DISCUSSION

It is already known that the Cl^--current of the anion channel which is excreted by *Clavibacter michiganense ssp. nebraskense,* is a nonlinear function of voltage (6). Here, the detailed current measurements at different salt concentrations were performed with the aim at developing a functional model of the channel on the basis of the

TABLE 1 **Values of b and G_0 obtained from the fitting of the data in Fig. 2, measured in lipid "C" and lipid "N," per Eqs. 2 and 3**

	Lipid "C"		Lipid "N"	
[KCl]	b / V^{-1}	G_0 / pS	b / V^{-1}	G_0 / pS
3.0 M KCl	7.8	19.0	6.7	18.8
1.8 M KCl	6.7	18.1	6.7	17.0
0.8 M KCl	6.5	16.3	6.5	14.5
0.3 M KCl	5.3	13.8	6.0	10.1
0.1 M KCl	5.4	8.1		
0.03 M KCl	2.9	4.8		

reaction-rate and the Nernst–Planck continuum theories. Due to the limited knowledge of the channel structure, molecular correlations with the functional properties cannot yet be made.

Voltage dependence. The increase of the conductance with V_m, as expressed in Eq. 3, is hardly caused by a continuous increase of the pore size, since we are dealing with small molecular dimensions. In addition, only for large water-filled pores the conductance is expected to be proportional to the cross-section of the pore. Furthermore, a decrease or even a reversal of the anion/cation-selectivity with increasing conductance, as was reported for alamethicin pores (9), was not observed with the CAC. Instead, a conformational two-substate model for the open pore, which was proposed to generally describe voltage dependent conductance changes (10), can be applied. In this model it is assumed that the transition frequency between the main open state $G(\tau_o)$ and at least one less conducting substate or closed state $G(\tau_c)$ is so high, that a single transition cannot be resolved. Thus, by reducing the time constant (τ_c) of a closing gap (flicker) or by increasing the mean open time (τ_o) of the (short) channel subevents, the *apparent* (average) conductance of the channel events

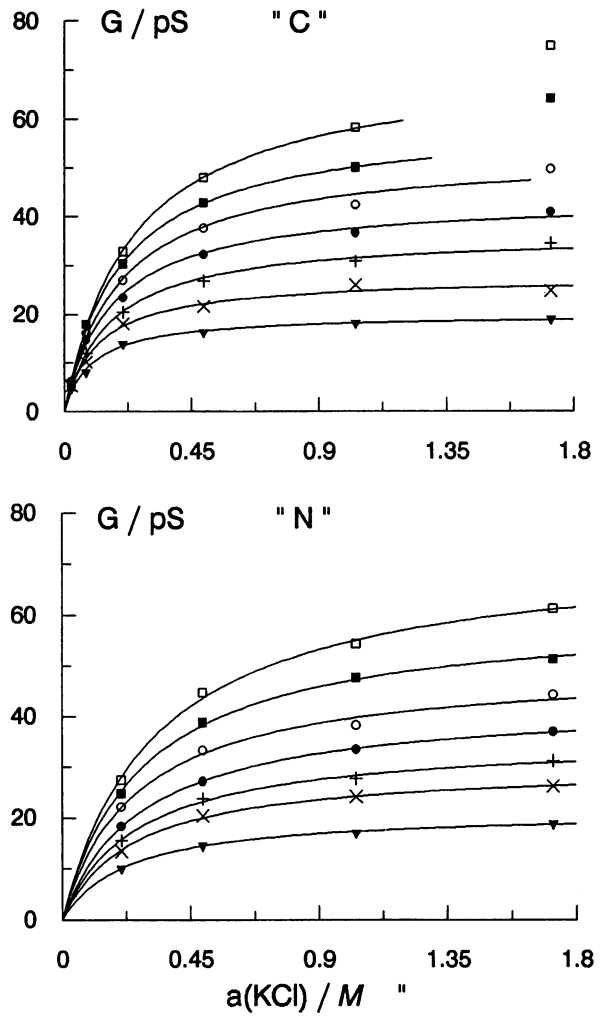

FIGURE 3 Chloride conductance (G) of the CAC as a function of KCl activity at various voltages (V_m). "C" and "N" denote the charged lipid C and the uncharged lipid N, respectively. The data were fitted by Eq. (4) of the text. The results are given in Table 3. The conductance-values at V_m = 0 mV were taken from the intercepts in Fig. 2 *B, D*. V_m: ■ 175 mV, □ 150 mV, ○ 125 mV, ● 100 mV, + 75 mV, × 50 mV, ▼ 0 mV.

$$G = G(\tau_o)\tau_o/(\tau_o + \tau_c) + G(\tau_c)\tau_c/(\tau_o + \tau_c) \qquad (7)$$

is increased. If $\tau_o \ll \tau_c$, $\tau_o/(\tau_o + \tau_c) = \tau_o/\tau_c$ and if $G(\tau_c) = 0$, we obtain

TABLE 2 **Single channel conductance after addition of large buffer anions in % of the values measured with standard buffer (5 mM PIPES, pH 6.8, and 300 mM KCl)**

Buffer anion	%conductance		
HEPES, pH 8.1, 450 mM			
cis + *trans*	70	60	35
cis	90	115	115
trans	100	80	45
HEPES < 0.25 mM			
cis + *trans*	100	100	100
PIPES, pH 6.8			
450 mM, *trans*	55	40	15
150 mM, *trans*	70	65	40
100 mM, *cis* + *trans*		75	55

TABLE 3 **G_{max}- and $K_{0.5}$-values obtained from the fitting of the data in Fig. 3, per Eq. 4**

	Lipid "C"		Lipid "N"	
V_m	G_{max} / pS	$K_{0.5}$ / M	G_{max} / pS	$K_{0.5}$ / M
175 mV	71.4	0.24	72.7	0.33
150 mV	59.8	0.20	60.4	0.29
125 mV	52.9	0.19	49.8	0.27
100 mV	43.6	0.17	42.7	0.26
75 mV	36.3	0.16	35.5	0.26
50 mV	27.5	0.12	30.1	0.25
0 mV	19.9	0.10	21.1	0.23

$$G = G(\tau_o) \cdot K(V_m). \quad (8)$$

Note that the mean lifetimes τ_o and τ_c are the reciprocals of the rate constants, $k_o = (\tau_c)^{-1}$ and $k_c = (\tau_o)^{-1}$ of the equilibrium reaction $C \rightleftarrows O$ between the closed (C) and the open (O) state and $K(V_m) = k_o/k_c = \tau_o/\tau_c$ is the equilibrium constant. Because $K(V_m) = \exp(-\Delta G^{\ominus}(V_m)/RT)$ is connected with the standard value of the molar electrochemical Gibbs free energy change of the reaction, $\Delta G^{\ominus}(V_m) = \Delta G^{\ominus}(0) + \Delta G^{\ominus}_{el}$, where $\Delta G^{\ominus}(0)$ refers to $V_m = 0$ and $\Delta G^{\ominus}_{el}$ is the (reversible) molar electric work, we obtain $K(V_m) = K(0) \exp(-\Delta G^{\ominus}_{el}/RT)$. Eq. 8 can be rewritten as

$$G = G_0 \cdot \exp(-\Delta G^{\ominus}_{el}/RT), \quad (9)$$

with $G_0 = G(\tau_o) \cdot K(0)$. The factor b in Eq. 3 is related to $\Delta G^{\ominus}_{el}$ by $b = -\Delta G^{\ominus}_{el}/(V_m RT) = -\rho z_g F/RT$. The product ρz_g of the "gating charge number" z_g and the "electrical distance" $\rho = \Delta V_m/V_m$ of the charge between two conformational substates can be calculated from the results in Table 1. For example, for $b = 6\ V^{-1}$, $|z_g| = 1$ and $RT/F \simeq 0.025$ V at $T = 293$ K, we obtain $|\rho| \simeq 0.15$; ρ thus denotes the fraction of the membrane voltage V_m, which is crossed by a (minimum) gating charge (with $|z_g| = 1$).

The frequent closing gaps and the large increase of the noise in the open state (Fig. 1) are in favor of such a two-state flicker (2SF) model for the open period of a channel. In addition it was shown that the average number of open channels also depends on voltage (6). The 2SF-model also infers that the conductance $G(\tau_o)$ is considerably larger than the average conductance, probably $G(\tau_o) > 100$ pS at physiological ion concentrations. However, the conductance of strongly ion-selective channels is generally below this value. It was therefore challenging to describe the single channel voltage dependence *without* the assumption of different conformational states—by the geometry (energy profile) of the pore. An interesting alternative to the 2SF-model comes from the reaction-rate theory, which is often used to describe ion channel conduction (11, 12).

Two-barrier, one-site (2B1S) rate theory model. The 2B1S-model is the simplest model of the Eyring rate theory that can be applied to ion channels. Although the real energy profile of a channel is probably much more complicated, the model has proven to describe the essential features of ion permeation through the acetylcholine receptor channel (12, 14). A detailed description of the model is given in (8) and (15); see also Fig. 6. In the 2B1S-model, the steady-state assumption for the intermediate state AS (see the reaction scheme in Fig. 6) of transient binding of the anion A^- in the channel yields the rate expression for the current (8)

$$I = e \frac{k_{-1}k_{-2}y[A]_{trans} - k_{+1}k_{+2}y[A]_{cis}}{k_{+2} + k_{-1} + k_{-2}y[A]_{trans} + k_1 y[A]_{cis}}. \quad (10)$$

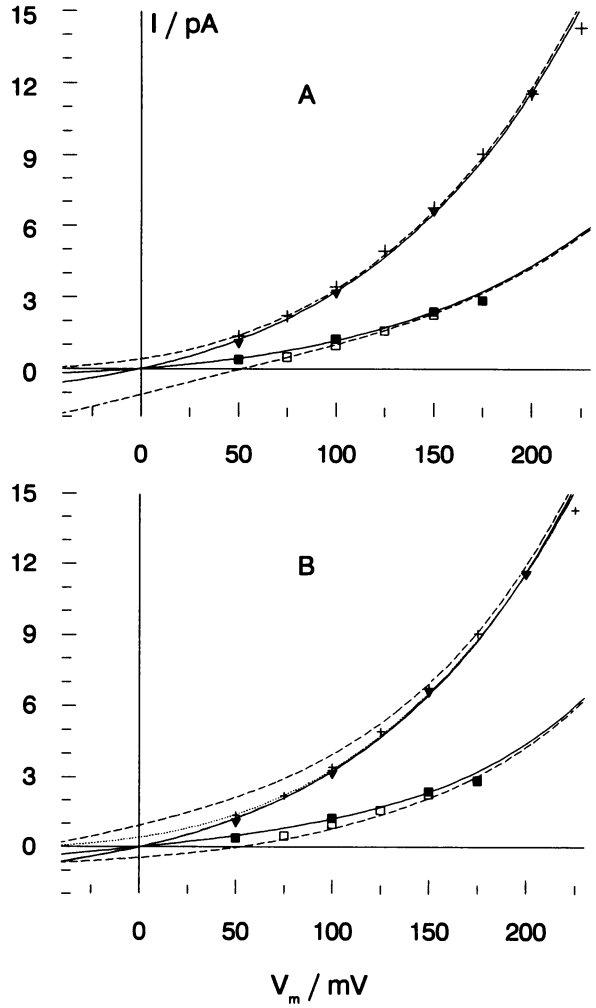

FIGURE 4 Chloride currents in the presence of ion gradients as a function of voltage (V_m). (A) 2SF-model (GHK): the current voltage curves were fitted according to Eq. 6. The values of G_0 and b relate to the concentration of KCl on the *trans*-side of the membrane, which were determined for $[KCl]_{trans} = [KCl]_{cis}$ (Table 1). Since the intercept I_0 at $V_m = 0$ depends on G_0, I_0 is different for the (+) and (−) gradient. (B) 2B1S-model: the data were fitted using Eq. (13) and the parameters of Table 4. [KCl]: + 0.1 M *cis*, 1 M *trans*; ▼ 1 M *cis* = *trans*; ■ 0.1 M *cis* = *trans*; □ 1 M *cis*, 0.1 M *trans*. Curves: full lines, symmetric solutions; broken lines, ion gradients; dotted line in (B) refers to data set 1 M (2) of Table 4 (no saturation) and (+) gradient.

Here, k_i are the rate coefficients, y is the activity coefficient, and [A] is the concentration of the permeant anion, respectively; e is the elementary charge. According

TABLE 4 **Values for a_i and δ obtained from the fitting of the data in Fig. 4 with Eq. 13, taking also into account the $K_{0.5}$-values (Saturation was not considered in (2))**

[KCl]/M	a_1	a_{-1}	a_2	a_{-2}	δ
0.1	10.8	13.1	14.2	11.9	0.1
1	10.7	13.0	14.1	11.8	0.2
1 (2)	13.9	10.6	9.6	12.9	0.25

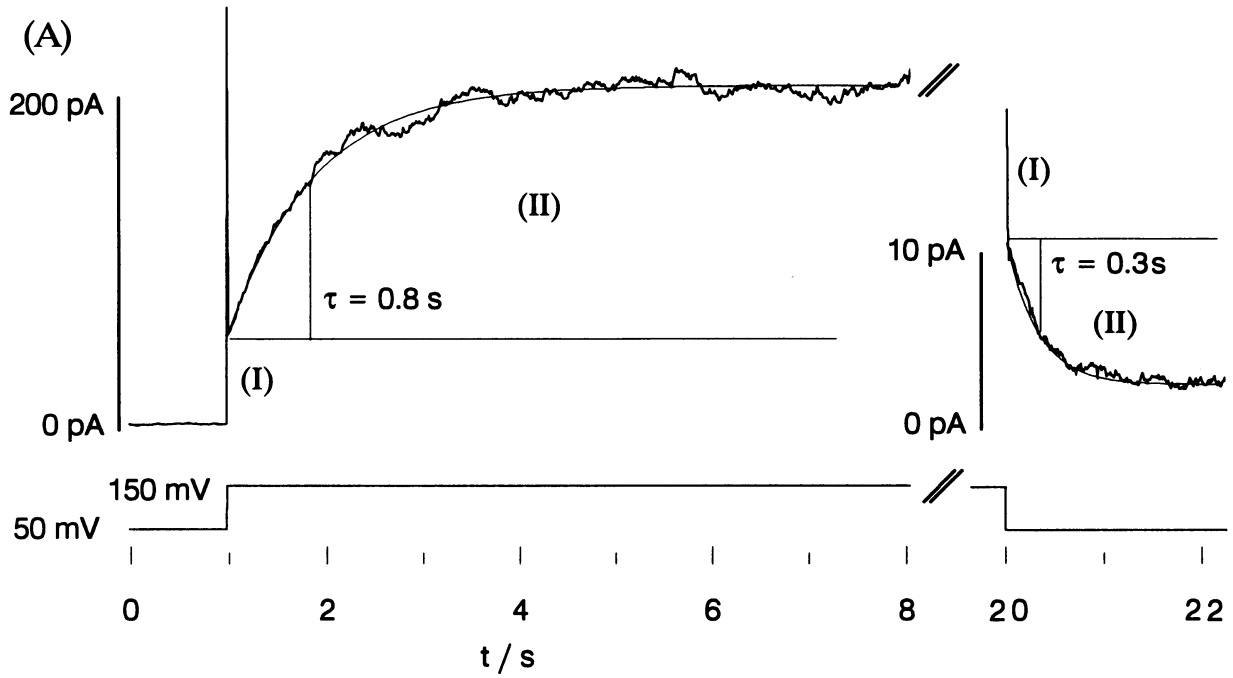

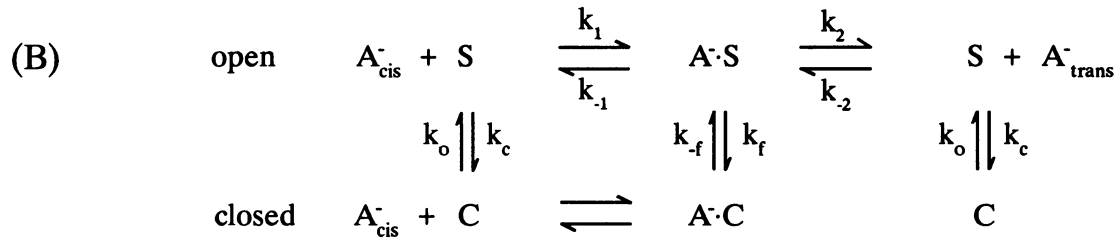

FIGURE 5 Current relaxations after a voltage jump. (*A*) The relaxation curves are averages of 10 measurements. τ is the relaxation time of the single exponential fit. The symmetrical bath solution contained 10 mM Hepes, pH 7.0, and 300 mM NaN_3. Note that the current scale on the right-hand side is enlarged. (*B*) Kinetic model: the slow phase II of the current relaxation (τ_{II} = 0.8 s at 150 mV and τ_{II} = 0.3 s at 50 mV) is most likely related to the opening and closing of the channel ensemble with $\tau^{-1} = k_o + k_c$, in terms of the corresponding rate coefficients. The fast, not resolvable component *I* is determined by the transport kinetics of the permeant ions (*horizontal arrows*). Possibly the flickering of the channel (k_f, k_{-f}) is also contained in the phase I. The rate coefficients k_1, k_{-1}, and k_2, k_{-2} describe the binding and dissociation, respectively, of the anion A^- to and from the channel-site S.

to absolute rate theory, the rate coefficient (k_i) of the i-th transition step between two states is

$$k_i = \nu_i(k_B T/h)\exp(-\Delta^{\#}G_i^{\ominus}(V_m)/RT), \qquad (11)$$

where k_B is the Boltzmann constant, h is the Planck constant, ν_i is the empirical transmission coefficient, and $\Delta^{\#}G_i^{\ominus}(V_m) = \Delta^{\#}G_i^{\ominus}(V_m = 0) + \Delta^{\#}G_{i,el}^{\ominus}(V_m)$ is the (molar) standard value of the electrochemical Gibbs free energy change associated with the preequilibrium between the well-state and the peak of the barrier to which the ion jumps. See Fig. 6. Substitution of the definition $a_i = \Delta^{\#}G_i^{\ominus}(V_m = 0)/RT$ and $\Delta^{\#}G_{i,el}^{\ominus}(V_m) = zF\Delta V_{m,i} = -uV_m\rho_i RT$ yields

$$\Delta^{\#}G_i^{\ominus}(V_m)/RT = a_i - uV_m\rho_i. \qquad (12)$$

Similar to the analysis of the V_m dependence of the conductance, a fractional electrical distance $\rho_i = \Delta V_i/V_m$ is introduced. If Eq. 12 is inserted into Eq. 11 and if we set $\rho_3 = \delta$ (Fig. 6) and all the remaining $\rho_i = (1 - \delta)/3$, Eq. 10 is rearranged to

$$I = \chi \cdot \frac{\exp(-a_{-1} - a_{-2} + 2uV_m(1-\delta)/3)y[A]_{trans}}{\exp(-a_{+2} - uV_m\delta) + \exp(-a_{-1} + uV_m(1-\delta)/3)} \cdot \frac{-\exp(-a_{+1} - a_{+2} - uV_m(\delta + (1-\delta)/3)y[A]_{cis}}{+\exp(-a_{-2} + uV_m(1-\delta)/3)y[A]_{trans} + \exp(-a_{+1} - uV_m(1-\delta)/3)y[A]_{cis}}. \qquad (13)$$

In Eq. 13, the factor $\chi = \chi_i = e \cdot \nu_i \cdot (kT/h) = e \cdot (kT/h)$ combines all the preexponential factors of Eq. 11. For channel analyses the transmission coefficient is usually taken as $\nu_i = 1$ (11). In contrast to the continuum theory *I–V* curves generated with the simple 2B1S-model are inherently nonlinear and yield a voltage dependent con-

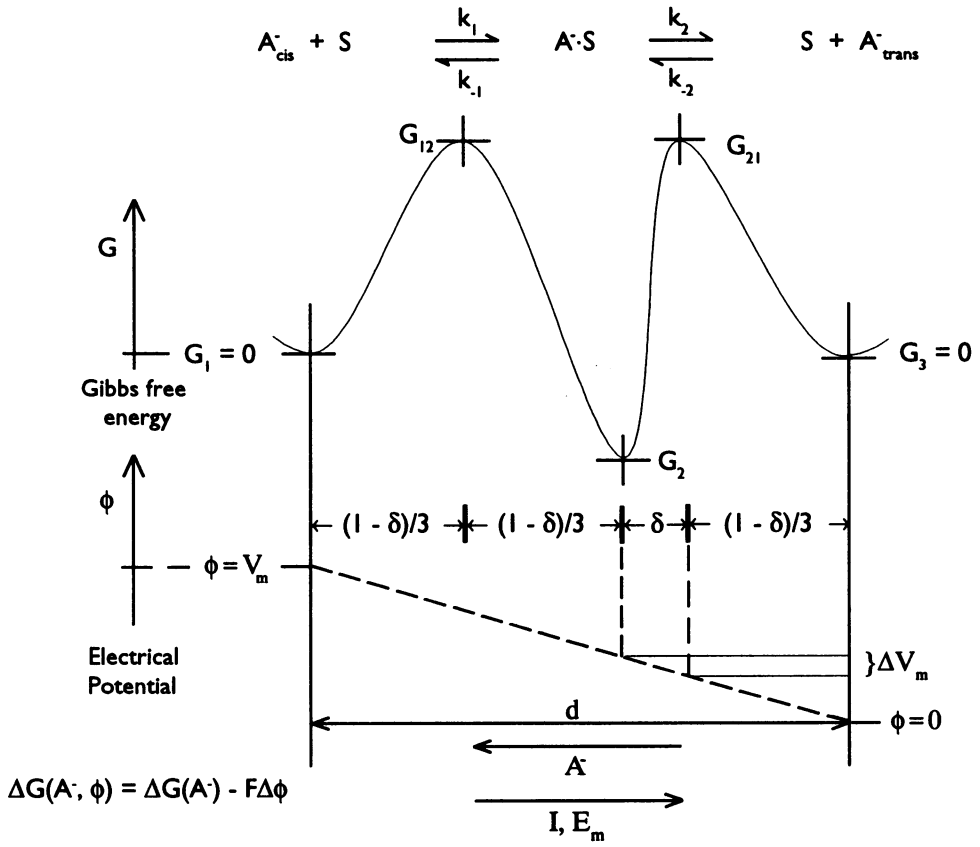

FIGURE 6 Two-barrier, one-site model (2B1S, reaction-rate theory). Reaction model for the anion transport in terms of the Gibbs free energy (G) and the electrical potential (ϕ) within the membrane channel length d. One barrier is asymmetric, to make the channel rectifying. V_m is the trans-membrane voltage, see Eq. (1) and $E_m = V_m/d$ the mean electrical field strength across the membrane. $\delta = \Delta V_m/V_m$ is the "electrical distance" between the binding-site S and the second barrier at G_{21}; A^- denotes a permeant anion and k_i is the rate coefficient of the i-th transition step. $\Delta G(A^-, \phi)$ is the potential dependent electrochemical Gibbs free energy change, $\Delta G(A^-)$ the conventional (isobaric, isothermal) Gibbs free energy change at $V_m = -\Delta\phi = 0$, and $F\Delta\phi$ is the reversible molar electrical work for the anion transport (note that $z = -1$).

ductance without a conformational change (Only for an infinite number of uniform barriers does the I–V relation follow the GHK-current equation (8)). Current rectification can be achieved by an asymmetry in the height of the barrier as well as by an asymmetry in the electrical distances; here δ has to be <0.25. The smaller is δ, the lower is the current driven by negative voltage.

To fit the I–V data in Fig. 4 we first generated an energy profile by fitting the voltage dependent $K_{0.5}$-values (Table 3) with appropriate rate constants k_i or transition energy terms a_i, respectively (see Eqs. 13 and 14; data not shown), in accordance with the concentration dependence of the channel conductance. The I–V curves were then obtained using only two variables: namely δ and an energy barrier increment Δa_i. For the ion gradients the same parameter values were used as for the corresponding symmetric ion concentrations. The "gradient curves" describe the data less satisfactorily at low values of V_m. In contrast to the 2SF-model, the value for the permeability (or $G/a(Cl^-)$) is not constant (due to saturation). Since we have used the term ($G/a(Cl^-$, *trans*) for the fittings with the 2SF-model, it appears that the saturation of the binding sites is mainly governed by the ions on the trans side. Correspondingly, the size of the intercept on the current axis is different for the (+)gradient and the (−)gradient. When the data were fitted with the 2B1S-model without saturation, the calculated curves matched those of the 2SF-model. The resulting energy profile (see data set (2) in Table 4), however, is not compatible with the saturation of the channel. (The differences may vanish with an extended rate theory model, e.g., with two different binding sites. However that is beyond the scope of this investigation.)

Current saturation. In the symmetric case of $[A]_{cis} = [A]_{trans} = [A]$, and after formal expansion with the term $(k_{-2} + k_1)^{-1}$, Eq. 10 obtains the suggestive form:

$$I = e\frac{(k_{-1}k_{-2} - k_{+1}k_{+2})}{(k_{-2} + k_1)} \times \frac{y[A]}{\{(k_{+2} + k_{-1})/(k_{-2} + k_1)\} + y[A]}. \quad (14)$$

It is readily seen that the rate coefficients can be combined to $G_{max}(V_m)$ and $K_{0.5}(V_m)$ of the simple saturation function in Eq. 4, where obviously $a = y[A]$.

Deviations of the data from the theoretical binding curve (Eq. 2) as found for the AChR at low salt concentrations were interpreted with a charged channel vestibule increasing the effective concentration of the permeant ions at the channel entrance and decreasing the apparent $K_{0.5}$ (14). The analysis of the K^+-binding of the AChR yielded $K_{0.5}$ = 74 mM compared to $K_{0.5}$ = 170–260 mM for the anion binding site of the CAC. The data of the anion channel can be satisfactorily fitted with Eq. 2 over the whole concentration range, indicating the absence of a charged channel vestibule.

Since the $K_{0.5}$-values calculated from the data obtained for neutral lipids were larger than those for charged lipids, a direct electrostatic effect of the lipids on the conductance can be excluded. An indirect charge effect of the lipid, causing conformational changes of the protein moiety, is therefore more probable.

Independent of the theoretical model used, a measurable current is expected from the intercept in Fig. 2 *B, D, F* at $V_m = 0$ and in the presence of a salt gradient. Since there were no detectable single-channel events under these conditions, we conclude that there is a very low probability for channel opening at low membrane voltage (6). Therefore the reversal potential cannot be experimentally determined. Nevertheless, the high anion selectivity, as determined by ion exchange (6), is in agreement with the results obtained by curve fitting of the present data.

Voltage dependence of fluoride conductance. Whereas the chloride current is only weakly reduced, even at higher concentrations of the buffer, the buffer has a considerable effect on the current carried by fluoride (Table 2 and Fig. 2 *F*). The blocking events are reflected in the increased channel noise (Fig. 1 *B*). As there is no current maximum at buffer concentrations ≤ 0.5 mM, it appears that the channel block of HEPES and PIPES (1 or 2 negative charges in the (fully) deprotonated form) is voltage dependent, as was described for the block of sodium current by protons (8), and the buffer anions account for the anomalous *I–V* curve of fluoride. If the blocking anion B is nonpermeant, a direct competition of B for the channel binding site with the permeant anions may be modeled by a simple rapidly equilibrating binding of B. In this case $K_{0.5} = (k_{+2} + k_{-1})/(k_{-2} + k_{+1})$, per Eqs. 4 and 14, is replaced by the apparent dissociation constant K_A for the permeant anion A, given by

$$K_A(V_m) = K_{0.5}(V_m) \cdot (1 + K_B^{-1}(V_m)[B]) \qquad (15)$$

where $K_B(V_m)$ is the voltage-dependent dissociation constant of the blocker and $K_{0.5}(V_m)$ is $K_A(V_m)$ at B = 0.

At V_m = 50 mV, where the channel blocking of the buffer is less pronounced, the conductances for fluoride and chloride have about the same value (~22 pS at 1 M). However, the values $K_{0.5}$ = 1.5 M and G_{max} = 76 pS for fluoride, which were evaluated from the conductance data in Fig. 2 *F*, are much higher than those for chloride ($K_{0.5}$ = 0.12 M and G_{max} = 27.5 pS). Both, a large $K_{0.5}$ and a large G_{max} are indicative for a weak binding of F^- in the channel and concomitant lower ability to compete with the buffer anions for the binding site. In analogy to the Eisenman sequences (8) the increase in the halide conductance from iodide to chloride supposes a large degree of dehydration of the anions in the channel. Corresponding to the lower binding energy, this condition is not expected for fluoride.

Voltage jumps. If the rectification of the anion channel really is based on the asymmetry of the energy barriers, the relaxation time of the single channel conductance (phase I) depends on the anion exchange rates, which are too fast to be resolved. The larger relaxation time (τ_{II} = 0.8 s), which can be assigned to an increase in the average number of open channels after a voltage jump, may be associated with a larger conformational change or even a reorganization of the channels in the lipid bilayer.

In conclusion, the voltage dependence of the CAC can be quantitatively described either by the 2SF-model and the continuum theory, or by the 2B1S-model with asymmetric barriers. As deduced from the voltage dependent current saturation, the asymmetry is mainly given by the different size of the barriers and to a lower extent by the electrical distances, which determine the electrical work. Thus, we have shown, that a voltage dependent conformational change is not necessary to describe the anion current data. However, the data suggest that fluctuations exist between different channel states. In order to decide whether the flickering contributes to the asymmetry of the *I–V* curve of the single channel, noise analysis would be necessary (16, 17). This, however, requires an additional technical setup and is planned for a future investigation.

We thank Prof. R. Eichenlaub and B. Fahrenholz for providing samples of the CAC.

This work was supported by the Deutsche Forschungsgemeinschaft under the program grant SFB 223, CO2.

Received for publication 1 April 1992 and in final form 11 September 1992.

REFERENCES

1. Wysong, D. S., A. K. Vidaver, H. Stevens, and D. Stenberg. 1973. Occurrence and spread of an undescribed species of *Corynebacterium* pathogenic on corn in the western corn belt. *Plant. Dis. Rep.* 57:291–294.
2. Rai, P. V., and G. A. Strobel. 1968. Phytotoxic glycopeptides produced by *Corynebacterium michiganense* I. Methods of preparation, physical and chemical characterization. *Phytopathology.* 59:47–52.
3. Vogel, P., B. A. Stynes, W. Coackley, G. T. Yeoh, and D. S. Petterson. 1982. Glycolipid toxins from parasitised annual ryegrass: a comparison with tunicamycin. *Biochem. Biophys. Res. Commun.* 105:835–840.
4. Van Alfen, N. K., and B. D. McMillian. 1982. Macromolecular

plant-wilting toxins: Artifacts of the bioassay method. *Phytopathology.* 72:132–135.

5. Krämer, R. and H.-U. Leistner. 1986. Physiological and cytological aspects of action of the toxin from *Corynebacterium michiganense pv. michiganense* (Smith) Jensen on the host-plant. *Zentralbl. Mikrobiol.* 141:437–451.
6. Schürholz, T., M. Wilimzig, E. Katsiou, and R. Eichenlaub. 1991. Anion channel forming activity from the plant pathogenic bacterium *Clavibacter michiganense ssp. nebraskense. J. Membr. Biol.* 123:1–8.
7. Schindler, H. 1980. Formation of planar bilayers from artificial or native membrane vesicles. FEBS (*Fed. Eur. Biochem. Soc.*) Lett. 122:77–79.
8. Hille, B. 1984. Ionic Channels of Excitable Membranes. Sinauer Associates Inc., Sunderland, Eng. 226–302.
9. Hanke, W., and G. Boheim. 1980. The lowest conductance state of the alamethicin pore. *Biochim. Biophys. Acta.* 596:456–462.
10. Läuger, P. 1985. Ionic channels with conformational substates. *Biophys. J.* 47:581–591.
11. Dani, J. A., and D. G. Levitt. 1990. Diffusion and kinetic approaches to describe permeation in ionic channels. *J. Theor. Biol.* 146:289–3011.
12. Levitt, D. G. 1986. Interpretation of biological ion channel flux data—reaction-rate versus continuum theory. *Annu. Rev. Biophys. Biophys. Chem.* 15:29–57.
13. Dani, J. A., and G. Eisenman. 1984. Acetylcholine-activated channel current-voltage relations in symmetrical Na^+ solutions. *Biophys. J.* 45:10–12.
14. Dani, J. A., and G. Eisenman. 1987. Monovalent and divalent cation permeation in acetylcholine receptor channels. *J. Gen. Physiol.* 89:959–983.
15. Dani, J. A. 1986. Ion-channel entrances influence permeation. Net Charge, size, shape, and binding considerations. *Biophys. J.* 49:607–618.
16. Sigworth, F. J. 1985. Open channel noise. I. Noise in acetylcholine receptor currents suggests conformational fluctuations. *Biophys. J.* 47:709–720.
17. Heinemann, S. H., and F. J. Sigworth. 1988. Open channel noise. IV. Estimation of rapid kinetics of formamide block in gramicidin A channels. *Biophys. J.* 54:757–764.